

# Immunoelectron Microscopy Study of Polyamines Using a Newly Prepared Monoclonal Antibody against Spermidine: Use of a Mixture of Glutaraldehyde and Paraformaldehyde as a Cross-Linking Agent in the Preparation of the Antigen

Toshio Tanabe<sup>1</sup>, Masashi Shin<sup>2</sup> and Kunio Fujiwara<sup>2,\*</sup>

<sup>1</sup>Diagnostic Agent Development Office, Nippon Kayaku, 1-11-2 Fujimi, Chiyoda-ku, Tokyo 102-8172; and

<sup>2</sup>Department of Applied Life Science, Faculty of Engineering, Sojo University, Ikeda 4-22-1, Kumamoto 860-0082

Received January 8, 2004; accepted February 6, 2004

We developed a mouse monoclonal antibody (ASPD-19, IgG3 sub-isotype mAb) against spermidine (Spd) conjugated to bovine serum albumin (BSA) using a mixture of glutaraldehyde (GA) and paraformaldehyde (PFA)-sodium borohydride for applications in immunoelectron microscopic studies. The antibody specificity was evaluated by an ELISA binding test simulating the immunocytochemistry (ICC) of tissue sections. The ASPD-19 mAb is highly specific for Spd and Spm, almost the same degree to each, and can distinguish alterations in the chemical structure of other polyamine (PA) analogs, showing less than 3.2% cross-reaction with *N*<sup>1</sup>-acetylspermidine, acetylspermine, or *N*<sup>8</sup>-acetylspermidine. By an indirect immunoperoxidase method using the ASPD-19 mAb, PA-like immunoreactivities were observed in different tissues fixed with Karnovsky fixative (a mixture of GA and PFA) in combination with borohydride reduction. In contrast, immunoreactivity was very low in tissues when the borohydride reduction step was omitted. The PA-like immunoreaction was completely abolished by the adsorption of the ASPD-19 mAb with 100 µg/ml of Spd or Spm, but was inhibited little or none by other PA-related compounds or amino acids. A light microscopic ICC method using ASPD-19 produced immunostaining of PAs in certain cells in rat tissues with high biosynthetic activities (small intestine, pancreas and spinal cord). A pre-embedding immunoelectron microscopic study using rat spinal cord showed PA immunoreactivity located predominantly on free (polysomes) and attached ribosomes of the rough endoplasmic reticulum (Nissl bodies) in the cytoplasm of motor neurons. These results are in complete agreement with the results obtained by our recent ICC method using another mAb (ASPM-29) produced against GA-conjugated Spm.

**Key words:** glutaraldehyde, immunoelectron microscopy, Karnovsky, monoclonal antibody, paraformaldehyde, spermidine.

Abbreviations: PA(s), polyamines; Spd, spermidine; Spm, spermine; Put, putrescine; Cad, cadaverine; GA, glutaraldehyde; PFA, paraformaldehyde; ELISA, enzyme-linked immunosorbent assay; HRP, horseradish peroxidase; ICC, immunocytochemistry; BSA, HSA, bovine (human) serum albumin; mAb, monoclonal antibody; Spd-BSA, spermidine-bovine serum albumin conjugate.

Polyamines (PAs), spermine (Spm), and spermidine (Spd), and their precursor, putrescine (Put), have been implicated in numerous important biological processes including cell proliferation and growth (1–4). Immunocytochemical studies (ICC) of PAs will help in developing a better understanding of these functional roles by revealing the exact cellular and subcellular localization of endogenous PAs. We recently developed a PA ICC method that uses the combination of a monoclonal antibody (mAb), ASPM-29, produced against glutaraldehyde (GA)-conjugated Spm, and GA as a fixative (5). A mAb specific for Spm and Spd is extremely useful for determining their localization in a variety of cells and tissues in ICC

studies (6–7). The ASPM-29 mAb, which recognizes the antigen structure of Spm fixed with GA in PA ICC, allowed us for the first time to conduct an immunoelectron microscopic study of PAs. The results showed that PAs are predominantly located on free and attached ribosomes in the neurons of the rat medulla oblongata (8). This adds strong support to the results of PA biochemistry, which suggest PAs are closely involved in the processes of protein biosynthesis (1–4, 9, 10). PAs are also known to be involved in a wide variety of biochemical activities; for example, PAs interact with DNA and RNA, they stabilize membrane structures, and they have effects on the activities of many enzymes, *etc.* (for reviews see Refs. 4, 11–13). Thus, there is a possibility that PAs also occur in organelles other than ribosomes within cells. An ICC with a strong fixative consisting of a mixture of GA and paraformaldehyde (Karnovsky fixative) may reveal PA localization precisely in detail since the

\*To whom correspondence should be addressed. Tel: +81-963-26-3111 (Ext. 5251), Fax: +81-963-23-1331, E-mail: fujiwara@life.sojo-u.ac.jp

fixative has the advantage of being among the best for preserving histological structures, and has been used extensively in electron microscopic studies (14–16). In our previous study, however, the ASPM-29 mAb was found to be completely inert in PA ICC using the Karnovsky fixative. Thus, the present study was designed to prepare an mAb that can be used in PA ICC using the Karnovsky fixative. It is known from ICC studies of small-sized molecules that the best results can be expected when the epitope of the hapten-protein conjugate used for immunization closely resembles the fixed tissue antigen, since the antibody can precisely recognize not only the antigen structure, but also, in part, cross-linking sites with carrier proteins (5, 17–20).

In this report, we describe the production, specificity, and application of a mAb against Spd using a mixture of GA and paraformaldehyde (Karnovsky fixative) in conjugate production and tissue fixation. The present ASPD-19 mAb was used in immunoelectron microscopic studies with the Karnovsky fixative, and revealed PAs in the motor neurons of rat cervical spinal cord.

#### MATERIALS AND METHODS

**Chemicals**—Spermine (Spm), spermidine (Spd), putrescine (Put), cadaverine (Cad), *N*<sup>1</sup>-acetylspermidine (*N*<sup>1</sup>-Ac-Spd), *N*<sup>1</sup>-acetylspermine (Ac-Spm), *N*<sup>8</sup>-acetylspermidine (*N*<sup>8</sup>-Ac-Spd), acetylputrescine (Ac-Put), and *o*-phenylenediamine (OPD), in the form of hydrochloride salts, were purchased from Sigma Chemical Co., St. Louis, Mo., USA. *N*<sup>1</sup>,*N*<sup>12</sup>-diacetylspermine (2Ac-Spm) and *N*<sup>1</sup>,*N*<sup>8</sup>-diacetylspermidine (2Ac-Spd) were kind gifts from Dr. N. Seiler of Marion Merrel Dow Research Institute, Strasbourg, France. The monoclonal antibody ASPM-29 used in this study was from the same batch used in a previous report (5). Goat anti-mouse gammaglobulin Fab' labeled with horseradish peroxidase (HRP) was purchased from MBL (Nagoya, Japan).

**Synthesis of Spd-BSA Conjugate (Antigen)**—A mixture of 4% PFA and 2.5% glutaraldehyde was prepared basically according to the method of Karnovsky (14), and diluted 15-times with distilled water prior to use as a cross-linking agent. Spd 3HCl (5.0 mg) in 1.0 ml 1 M sodium acetate was incubated with 1.0 ml of a solution of the cross-linking agent for 30 s with stirring. To this reaction mixture was added 10 mg of carrier protein [bovine (BSA) or human serum albumin (HSA)] in 1.0 ml of sodium acetate, and the entire mixture was incubated for 30 min at room temperature with slow stirring. Then, 5 mg of solid sodium borohydride (Sigma) was added so that the double bonds were saturated. The coupling mixture was dialyzed for 8 h against several changes of 10 mM sodium acetate at 4°C. Insoluble materials were removed by centrifugation at 10,000 ×g for 10 min.

**Preparation of Anti-Spd mAb**—Five-week-old, female BALB/c mice were injected intraperitoneally with 100 µg of Spd-BSA conjugate emulsified in complete Freund's adjuvant (Difco). Subsequently, they received three injections of 50 µg of the conjugate alone at two week intervals. Following immunization, antisera were collected, and antibody titers were evaluated with an enzyme-linked immunosorbent assay (ELISA) as described below. The mouse with the best immune response was selected

for hybridization. The mouse received a fifth i.p. booster injection and was sacrificed 4 days later.

**Cell Fusion and Cloning**—The spleen cells ( $2 \times 10^8$ ) from the immunized mouse and  $3 \times 10^7$  myeloma cells (P3/NS-1) were fused with the help of polyethylene glycol according to the method of Kato *et al.* (21). Cells suspended in HAT medium were plated out in 96-well tissue culture plates (Corning) at a density of  $10^5$  cells per well in which  $10^5$  feeder cells had been plated. From 10 to 20 days post-fusion, the wells were screened for reactivity using an ELISA method, as described below. Limiting dilutions of positive cultures were carried out two or three times to obtain monoclonality, and sub-isotyping of the mAbs was performed using a Mouse Monoclonal Sub-isotyping kit (American Qualex Int., La Mirada, Calif., USA).

**ELISA Method**—ELISA was performed similarly to our previous method for anti-spermine (Spm) mAbs (5). In screening clones for the production of antibody against Spd-BSA, wells in microtiter plates were coated with the Spd-HSA conjugate (10 µg/ml) for 30 min at room temperature. The wells were then incubated overnight at 4°C with antiserum (diluted 1:3,000), hybridoma culture supernatant, or ascites fluid (diluted 1:100,000), followed by goat anti-mouse IgG labeled with HRP (diluted 1:2,000) for 1 h at 25°C. The amount of enzyme conjugate bound to each well was measured using *o*-phenylenediamine as a substrate, and the absorbance at 492 nm was read with an automatic ELISA analyzer.

**ELISA Binding Test**—The procedure was done according to our previous method (5, 22). Wells in a microtiter plate coated with poly-L-lysine (30 µg/ml) were activated with 2.5% GA at pH 10.0 for 1 h. Test compounds including Spd, Spm, Put, Cad, L-ornithine, L-lysine, *N*<sup>1</sup>-acetylspermidine (*N*<sup>1</sup>-Ac-Spd), *N*<sup>1</sup>-acetylspermine (Ac-Spm), *N*<sup>8</sup>-acetylspermidine (*N*<sup>8</sup>-Ac-Spd), *N*<sup>1</sup>,*N*<sup>12</sup>-diacetylspermine (2Ac-Spm), *N*<sup>1</sup>,*N*<sup>8</sup>-diacetylspermidine (2Ac-Spd), and acetylputrescine (Ac-Put) at various concentrations were added to the wells, and the plates were incubated for 1 h at 25°C. Excess aldehyde groups were blocked with 0.5% NaBH<sub>4</sub> for 10 min. The wells were further blocked with 1% skimmed milk for 1 h for protein binding sites, and then incubated overnight at 4°C with mAb hybridoma culture supernatant (diluted 1:100). The wells were then incubated with HRP-labeled anti-mouse IgG (1:2,000) for 1 h. The bound enzyme activity was then measured as described above.

**Animals**—Normal adult male Wistar rats (Otsu Exp. Animals; Nagasaki, Japan), body weight 200–250 g, were used in this study. The principles of laboratory animal care and specific national laws were observed. The animals were housed in temperature- and light-controlled rooms (21 ± 1°C and 12L:12D) and had free access to standard food and tap water.

**Immunocytochemistry (ICC)**—Under sodium pentobarbital (Abbott Lab.; North Chicago, IL, USA) (60 mg/kg) anesthesia, the rats were perfused intracardially with phosphate-buffered saline (PBS) at 50 ml/min for 2 min at RT, and then with a freshly prepared solution of 2.5% GA plus 4% PFA in 10 mM phosphate buffer at pH 7.2 for 6 min. Specimens from various tissues were post-fixed in the same fixative overnight at 4°C, and were subsequently embedded in paraffin in a routine way. The

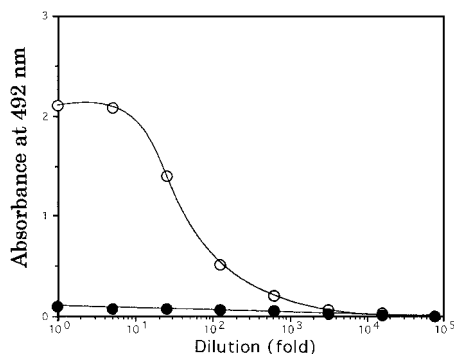


Fig. 1. **Dilution curve for ASPD-19.** Various dilutions of ASPD-19 were incubated in microtiter wells coated with spermidine (Spd)-BSA conjugate overnight at 4°C. The samples were analyzed by the procedure described for ELISA using horseradish peroxidase (HRP)-labeled goat anti-mouse IgG (1:2,000) as the second antibody. ASPD-19 (open circles), anti-histamine mAb AHA-2 (solid circles)

samples were sliced into 5- $\mu$ m-thick sections, treated with 0.2% NaBH<sub>4</sub> for 10 min, and incubated at 4°C overnight with primary mAb ASPD-19 at concentrations ranging from 10 to 50 ng/ml in 50 mM TRIS-HCl buffer, pH 7.4, containing 0.86% NaCl (TBS). The antibody concentrations were determined by a conventional “sandwich ELISA” method using chromatographically purified mouse IgG (Zymed Lab.; San Francisco, CA) as a standard. The sections were then incubated with goat anti-mouse IgG/Fab’ labeled with HRP (MBL; Nagoya, Japan) 1:200 for 1 h at 4°C. After rinsing with TBS, the HRP was exposed for 5–10 min to diaminobenzidine (DAB) and H<sub>2</sub>O<sub>2</sub>. The HRP substrate consisted of 10 mg of 3,3'-diaminobenzidine tetrachloride (Sigma) dissolved in 20 ml of 50 mM TRIS buffer, pH 7.4, supplemented with 20  $\mu$ l of 30% H<sub>2</sub>O<sub>2</sub> (Graham and Karnovsky 1966).

**Electron Microscopy**—The spinal cord, post-fixed with Karnovsky fixative, was cut into 50- $\mu$ m-thick sections with a Microslicer (Dosaka EM Co.; Kyoto, Japan). The sections were treated in the same manner as described above for light microscopy except that they were incubated with the primary and secondary antibodies for 48 and 36 h, respectively. The color specimens prepared by the DAB reaction were rinsed first with TRIS-HCl buffer, pH 7.4, and then with cacodylate buffer, pH 7.4, for 30 min at RT. The sections were then fixed with 1.0% osmium tetroxide in 50 mM cacodylate buffer, pH 7.4, for 1 h at RT, and dehydrated in a series of graded ethanol solutions. After immersion in propylene oxide (Nacalai Tesque; Kyoto, Japan) (three times for 10 min each), the samples were immersed in a mixture (1:1) of propylene oxide and Epon 812 resin (Taab Lab.; Reading, Berks) for 2 h, and embedded in Epon 812 resin in a routine way. The regions to be studied were cut with a 2-mm diameter punch, mounted on Epon blocks and sectioned on a horizontal plane into ultrathin sections, which were then immediately observed in a JEM-1200 EX electron microscope (JEOL; Tokyo, Japan).

**Control Experiments**—In the Spd immunocytochemistry study, the specificity of immunostaining was ascertained by incubating control sections with (i) the secondary antiserum alone and (ii) ASPD-19 mAb pre-adsorbed with Spd at a concentration of 100  $\mu$ g/ml.

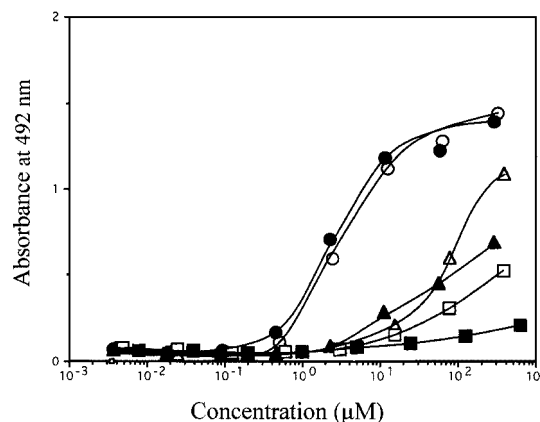


Fig. 2. **Reactivity of ASPD-19 as measured by its immunoreactivity in the ELISA binding test.** Activated wells prepared for the ELISA binding test were incubated with various concentrations of the following compounds: Spd (open circles), Spm (solid circles), N<sup>1</sup>-Ac-Spd (open triangles), N<sup>8</sup>-Ac-Spd (open squares), Ac-Spm (solid triangles), and Put (solid squares). The wells were then incubated with ASPD-19 mAb (1:50) followed by HRP-labeled goat anti-mouse IgG (1:2,000).

## RESULTS

**Antibody Response**—The immunogen Spd-BSA conjugate elicited the production of an anti-Spd antibody in each of the three mice. The antibody titers in the serum samples were examined by ELISA using Spd-HSA as a solid phase antigen in order to avoid the binding of antibodies raised against the carrier protein BSA. Titers were found to peak 2 weeks after the third booster injection.

**Production and Detection of mAb to Spd**—From the fusion experiment, 525 hybridoma lines were produced. It was found that only one hybridoma line secreted an antibody that bound to the Spd-HSA conjugate but did not recognize HSA, as determined by ELISA. This line continued to secrete antibodies in both culture supernatant and ascites fluids in mice.

**Sub-Isotyping of Subclones**—All subclones of the hybridoma obtained by limiting dilution were found to produce an antibody of the IgG3 sub-isotype.

**Antibody Dilution**—Microtiter wells coated with Spd-HSA conjugate (10  $\mu$ g/ml) were used to test for antibody binding using serial dilutions of ASPD-19 mAb (hybridoma culture supernatant). As shown in Fig. 1, significant binding activity was observed at antibody dilutions greater more than 1,000 fold. No antibody binding was seen with type-matched (IgG1) mAb of AHA-2, known to be specific for histamine (23).

**Evaluation of Antibody Specificity by ELISA Binding Test**—This test simulates the immunocytochemistry of tissue sections based on the principle of coupling the amino group of analytes to the wells of a microtiter plate activated with poly-L-lysine and GA, and incubating the wells by the indirect immunoperoxidase method (5, 22, 23). As shown in Fig. 2, analysis of the relationship between the concentration of each of the PAs applied to the wells and bound HRP activity produced dose-dependent saturation curves with Spd and Spm in the range of 1  $\mu$ M to 300  $\mu$ M. The dose of each analyte required for 0.75

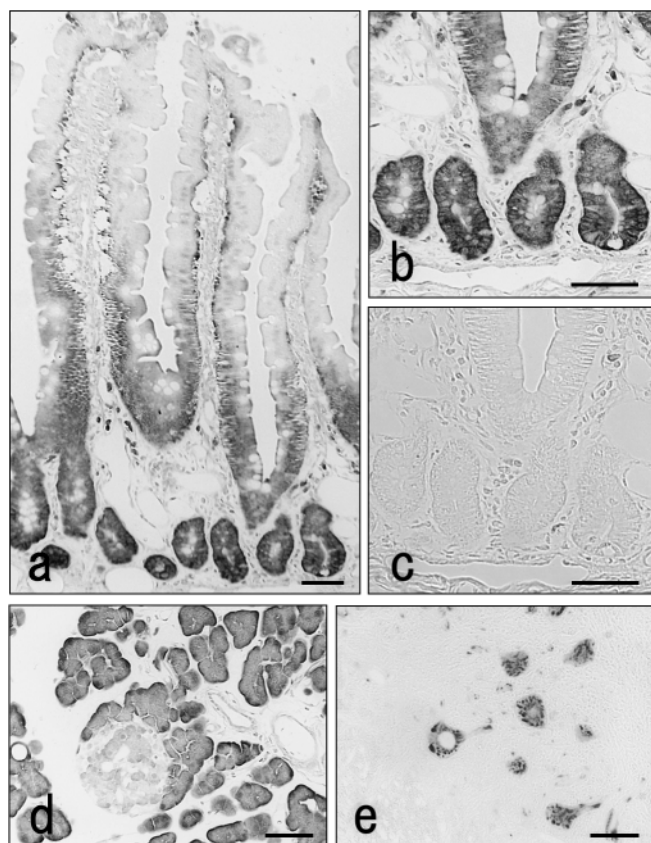


**Fig. 3. a–e: Rat small intestine, pancreas, and cervical spinal cord stained for polyamines by an immunocytochemical method using ASPD-19 mAb (indirect method).** (a) Duodenum: Strong immunostaining occurs in cells in the crypts of Lieberkuhn; the staining intensity decreases along the crypt-to-villus gradient. A magnified view of the lower part of crypts (b) was compared with a control specimen (c) in which spermidine (100  $\mu\text{g}/\text{ml}$ ) was added to the ASPD-19 antibody solution. (d) Pancreas: Immunostaining occurs in the basal cytoplasm of terminal portions of acinar cells, but only weak staining is evident in the cytoplasm of islet cells. (e) Motor neurons of the cervical spinal cord: Strong staining occurs in clusters in the cytoplasm, while no staining is seen in the nuclei of the neurons. Bars a–e 50  $\mu\text{m}$ .

of absorbance at 492 nm was determined from the curves and used as an index of the degree of immunoreactivity: this dose was 2.4  $\mu\text{M}$  for Spm, 2.9  $\mu\text{M}$  for Spd. Much weaker immunoreactions occurred with  $N^1$ -Ac-Spd (90  $\mu\text{M}$ ), Ac-Spm (>300  $\mu\text{M}$ ), and  $N^8$ -Ac-Spd (>300  $\mu\text{M}$ ). Almost no immunoreaction was seen with Put, Cad, L-ornithine, 2Ac-Spm, 2Ac-Spd, or Ac-Put at less than 1 mM. If the  $\text{NaBH}_4$  reduction step was omitted from the protocol, no antibody binding occurred at concentrations ranging from 0.1 and 600  $\mu\text{M}$  with any of the PAs or related compounds.

**Immunocytochemistry**—The usefulness of the ASPD-19 mAb for ICC was tested in some rat tissues. No significant staining was seen when the tissues were fixed with 4% PFA, 3.7% formalin, or 5% carbodiimide. Fixation with a mixture of 2.5% GA plus 2% PFA, or GA alone resulted in very slight immunostaining of certain cells. However, the latter two fixation methods, when combined with reduction of the tissues by  $\text{NaBH}_4$ , resulted in intense staining of such cells.

In the duodenal mucosa, the degree of immunostaining was highest in the cytoplasm of cells in the deep area of the crypts of Lieberkuhn and decreased gradually along the crypt- to villus tip cell gradient (Fig. 3, a and b). In the pancreas, immunoreaction for PAs was seen in the basal cytoplasm of pancreatic acinar cells, with very weak immunoreactivity in the cytoplasm of the islets of Langerhans (Fig. 3d). In the cervical spinal cord, strong PA immunoreactivity was observed in the cytoplasm and dendrites of the large nerve cells in the anterior column at all levels of the tissue. The patterns of PA immunostaining were either clustered masses or block-like (Fig. 3e). The middle and small-sized nerve cells in the gray matter were weakly immunostained (data not shown). Very weak or no staining was observed in the nuclei of all cell types, in glial cells, or in nerve fibers passing through the white matter and entering into the gray matter. Conventional immunocytochemical staining controls (second level controls) were all negative. The adsorption controls for ASPD-19 mAb showed that the addition of Spd-BSA conjugate at a concentration of 2  $\mu\text{g}/\text{ml}$  into the antibody abolished all staining. Free Spd also inhibited the immunoreaction, but at a much higher concentration (100  $\mu\text{g}/\text{ml}$ ) (Fig. 3c).

Immunoelectron microscopic examination of the large neurons in the anterior column at the cervical level of the spinal cord showed low magnification immunoreactivity in a number of clusters of rER (Fig. 4a), and higher magnification immunoreactive end deposits concentrated specifically and intensely in ribosomes attached to the membranes of rER, in free ribosomes (polysomes) clustered between cisternae, and in the polysomes widely spread throughout the entire cytoplasm (Fig. 4c). The nuclei, nucleoli, mitochondria, Golgi cisternae, Golgi vesicles, and lysosomes in the cytoplasm of perikaryons were devoid of PA immunoreactivity (Fig. 4, a and c). The axons, both myelinated and unmyelinated, and the synaptic vesicles in nerve endings around the neurons were completely PA-negative. The sections incubated with the preabsorbed mAb ASPD-19 showed no PA immunoreactivity (Fig. 4b). Additionally, neurons were also immunostained for PAs with the previously developed ASPM-29 mAb, providing exactly the same results as with the ASPD-19 mAb, but with rather poor morphology (Fig. 4d).

## DISCUSSION

We have previously undertaken immunoelectron microscopic studies of PAs employing ASPM-29 mAb, which was produced against GA-conjugated Spm (5). This antibody was very useful in PA ICC studies using GA as a fixative, because PAs, which are small molecules with a tendency to diffuse, can be fixed through covalent bonds *in situ* using this fixative. In addition, the mAb precisely recognizes not only the Spm of the antigen structure, but, also, in part, the sites of GA cross-linking with carrier protein (5–8). However, it was found that no immunoreaction with the ASPM-29 mAb occurred in PA ICC when GA was replaced by a mixture of GA and PFA (Karnovsky fixative), which is, in general, known to be a stronger fixative than GA alone, and which allows some of the best morphological observations in electron microscopic studies. This lack of immunoreactivity might be due to

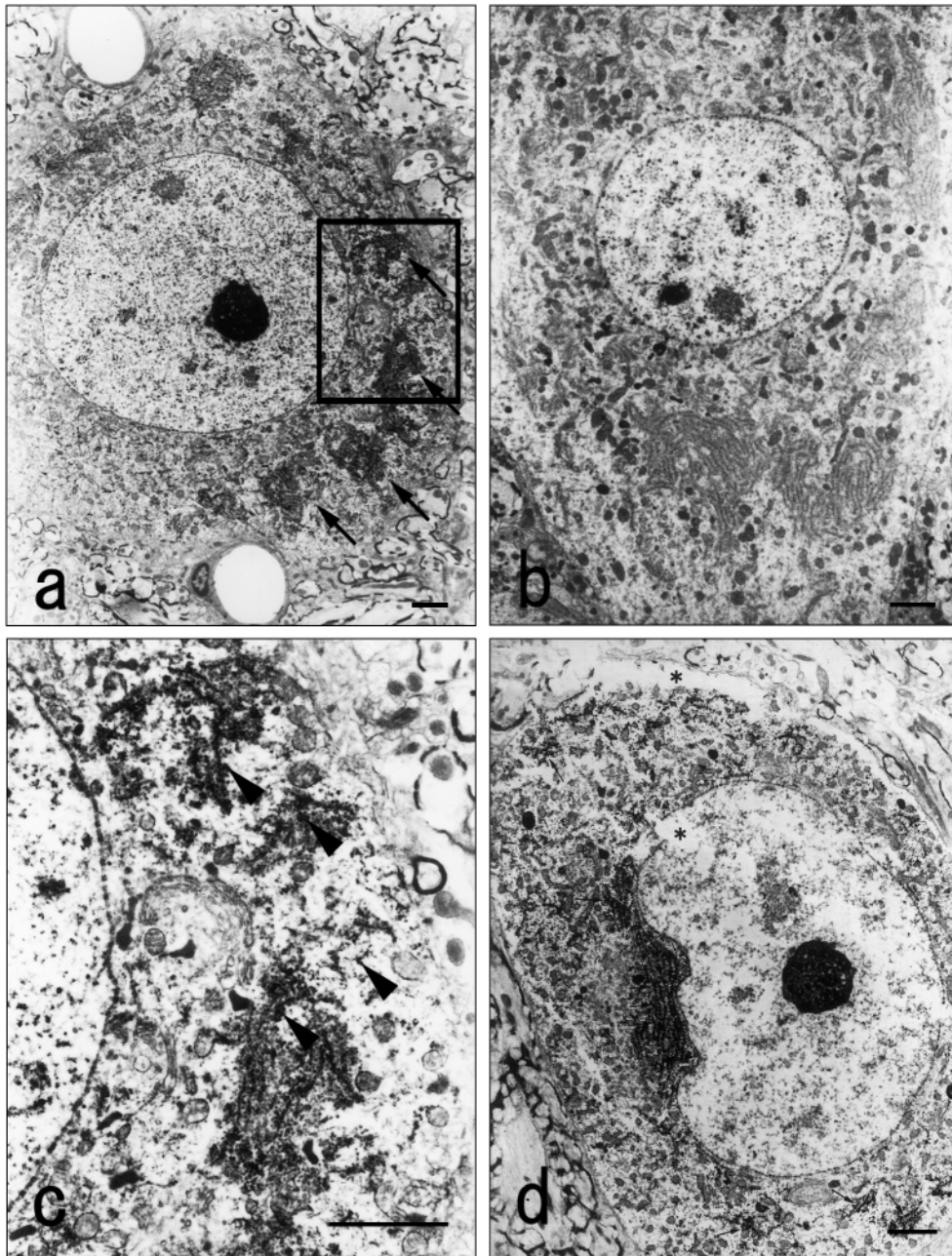


Fig. 4. **a-d: Immunocytochemical localization of PAs in a motor neuron in the cervical spinal cord.** (a) Strong immunoreactivity exists in the rER (arrows) in the cytoplasm. The nucleus and nucleolus in the neuron are PA-negative, as are the myelinated and unmyelinated axons and nerve endings around the neurons. (c) Higher magnification of the framed area in a, showing strong PA immunoreactivity on free (polysomes) and attached ribosomes

(arrowheads). The Golgi cisternae, Golgi vesicles, lysosomes and mitochondria are PA-negative. (d) Similar immunoreactivity of PAs occurred in the ribosomes (arrows) of a neuron stained with the ASPM-29 mAb, showing breakage (asterisks) in some parts. (b) The staining (seen in a) was completely abolished by the adsorption of the mAb with Spd (100 μg/ml). Bars a-d 2 μm.

changes in PA antigenicity that may occur *in situ* by the reaction of PAs at multiple amino groups with PFA included in the fixative. The present study was undertaken in order to study the relationship between the specificity of the antibody and the fixative effectively used in ICC, and to develop a mAb that can be used in immunoelectron microscopic studies using the Karnovsky fixative. Also, in our previous studies, we failed to prepare IgG-typed mAbs against Spd when it was conju-

gated via GA alone and used as an antigen, but rather produced IgM-typed mAbs, which are generally inappropriate to ICC.

Using a mixture of GA and PFA for Spd-conjugate preparation, we have now prepared and characterized a mAb against Spd. A large number of hybridomas were obtained, with 60% of the wells yielding colonies, but only one (ASPD-19, IgG3-type antibody) showed selective binding activity for Spd. This hybridoma showed a pro-

lific growth rate, so it was cloned, and three of the resulting subclones continued to secrete the IgG3 antibody.

With an ELISA system using the Spd-HSA conjugate as the solid phase antigen, the ASPD-19 mAb showed a high titer of binding activity. No antibody activity against the carrier HSA or HSA conjugated only with the Karnovsky fixative mixture was evident, demonstrating a lack of recognition. An ELISA binding test indicated that Spd and Spm react with the mAb to almost the same degree, followed by  $N^1$ -Ac-Spd, Ac-Spm, and  $N^8$ -Ac-Spd, each with a less than 3.2% cross-reaction value (Fig. 2). However, almost no cross-reaction occurred with Put, Cad, 2Ac-Spd, 2Ac-Spm, Ac-Put, or ornithine at concentrations below 600  $\mu$ M. In the binding test, the reduction process with  $\text{NaBH}_4$  was absolutely necessary for the Karnovsky fixative-conjugated Spd to retain antibody binding ability. In addition, another ELISA binding test, in which PAs and analogs conjugated on a solid phase were treated again with Karnovsky fixative followed by  $\text{NaBH}_4$ , demonstrated enhanced immunoreactivity with Spd and Spm, and to a lesser extent with the other analogs tested (data not shown). These results suggest the possibility that the ASPD-19 mAb was generated recognizing Spd-BSA conjugates in which Spd reacted with GA and/or PFA at multiple amino groups (both primary and secondary amino group) in the molecule, which were then reduced with  $\text{NaBH}_4$ , just as conjugation between PAs and Karnovsky fixative has been shown to occur during tissue fixation of PA ICC (5, 28).

For ICC applications,  $\text{NaBH}_4$  treatment, in combination with either Karnovsky fixation or GA alone, was absolutely necessary for the antibody-antigen reaction, consistent with the results of the ELISA binding test (Fig. 2). The light microscopic ICC results obtained in this study show strong PA-like immunoreactivity in the cytoplasm of cells not only in the cell proliferative zone, but also in the neighboring cell zone of the small intestine, in the basal cytoplasm rather than the apical cytoplasm of rat pancreas acinar cells, and in the cytoplasm and dendrites of the large nerve cells in the anterior column of the cervical spinal cord (Fig. 3, a, b, d, and e). The immunoelectron microscopic study also demonstrated that PAs are predominantly located on free (polysomes) and attached ribosomes of the rough endoplasmic reticulum (Nissl bodies) in the cytoplasm of the motor neurons of the rat spinal cord (Fig. 4, a and c). However, no immunoreaction was evident in the nuclei, axons, or nerve endings of the central nervous system. These results are in complete agreement with those obtained in our previous studies using the ASPM-29 mAb, thus adding support to our previous idea that PAs are closely involved in the translation processes of protein biosynthesis (5–8, 29). Also, this subcellular localization might well explain the light microscopic observation that PAs are abundant in the cytoplasm of active protein- or peptide-secreting cells of the pancreas, and rapidly proliferative cells in the intestinal epithelia. Comparing the results of ICC using the ASPD-19 and ASPM-29 mAbs, the morphological observations at the electron microscopic level were much better in the present ICC using the Karnovsky fixative than in the previous one using GA and the ASPM-29 mAb in combination (Fig. 4d) (8). On the other hand, the

antigenicity of PAs *in situ* in tissues seems to be less strong under the present conditions, possibly due to the fact that tissues are fixed more strongly with Karnovsky fixative than with GA alone, thus decreasing the permeability of the antibody into cells. This relationship in ICC between the strength of fixation and antigenicity is in general known to be contradictory (30). Also, each tissue fixes differently even under the same fixation conditions. In order to generalize the subcellular localization of PAs, we are now undertaking further immunoelectron microscopic investigations of tissues other than nerve tissues by changing the fixation conditions while using the present ASPD-19 mAb.

In conclusion, the ASPD-19 mAb was newly produced against conjugated-Spd using a mixture of GA and PFA as a cross-linking agent; this new mAb allowed us to carry out immunoelectron microscopic studies of PAs using a Karnovsky fixative. The present ICC results agree with those obtained in our previous study using the ASPM-29 mAb, showing that PAs are predominantly located on the ribosomes of rat neurons. Thus, this method should have potential for studies to further clarify the biological role of PAs in a variety of cells.

We are grateful to Tanaka H, Toyoda Y, Hirokawa H, and Sugimoto M for technical assistance throughout this study.

#### REFERENCES

1. Tabor, C.W. and Tabor, H. (1984) Polyamines. *Annu. Rev. Biochem.* **53**, 749–790
2. Pegg, A.E. (1986) Recent advances in the biochemistry of polyamines in eukaryotes. *Biochem. J.* **234**, 249–262
3. McCormack, S.A. and Johnson, L.R. (2001) Polyamines and cell migration. *J. Physiol. Pharmacol.* **52**, 327–349
4. Thomas, T. and Thomas, T.J. (2003) Polyamine metabolism and cancer. *J. Cell Med.* **7**, 113–126
5. Fujiwara, K. and Masuyama, Y. (1995) Monoclonal antibody against the glutaraldehyde-conjugated polyamine, spermine. *Histochem. Cell Biol.* **104**, 309–316
6. Fujiwara, K., Masuyama, Y., and Kitagawa, T. (1996) Immunocytochemical localization of polyamines in the gastrointestinal tracts of rats and mice. *Histochem. Cell Biol.* **106**, 465–471
7. Fujiwara, K., Bai, H., and Kitagawa, T. (1997) Polyamine-like immunoreactivity in rat neurons. *Brain Res.* **767**, 166–171
8. Fujiwara, K., Bai, H., Kitagawa, T., and Tsuru, D. (1998) Immunoelectron microscopic study for polyamines. *J. Histochem. Cytochem.* **46**, 1321–1328
9. Kakegawa, T., Hirose, S., Kashiwagi, K., and Igarashi, K. (1986) Effect of polyamines on *in vitro* reconstitution of ribosomal subunits. *Eur. J. Biochem.* **158**, 265–269
10. Kakegawa, T., Sato, S., Hirose, S., and Igarashi, T. (1986) Polyamine binding sites on *Escherichia coli* ribosomes. *Arch. Biochem. Biophys.* **251**, 413–420
11. Tabor, C.W. and Tabor, H. (1985) Polyamines in microorganisms. *Microbiol. Rev.* **49**, 81–99
12. Schuber, F. (1989) Influence of polyamines on membrane functions. *Biochem. J.* **260**, 1–10
13. Wallace, H.M., Fraser, A.V., and Hughes, A. (2003) A perspective of polyamine metabolism. *Biochem. J.* **376**, 1–14
14. Karnovsky, M.J. (1965) A formaldehyde-glutaraldehyde fixative of high osmolality for use in electron microscopy. *J. Cell Biol.* **27**, 137A–138A
15. Setoguchi, T., Inoue, Y., and Shin, M. (1985) Effects of short-term treatment with calcium on the parathyroid gland of the rat, under particular consideration of the alteration of storage granules. *Cell Tissue Res.* **240**, 9–17

16. Sykes, R.M., Spyer, K.M., and Izzo, P.N. (1997) Demonstration of glutamate immunoreactivity in vagal sensory afferents in the nucleus tractus solitarius of the rat. *Brain Res.* **762**, 1–11
17. Buijs, R.M., Geffard, M., Pool, C.W., and Hoorneman, E.M.D. (1984) The dopaminergic innervation of the supraoptic and paraventricular nuclei. A light and electron microscopic study. *Brain Res.* **323**, 65–72
18. Onteniente, B., Geffard, M., and Calas, A. (1984) ultrastructural immunocytochemical study of the dopaminergic innervation of the rat lateral septum with anti-dopamine antibodies. *Neuroscience* **13**, 385–393
19. Seguela, P., Geffard, M., Buijs, R.M., and Le Moal, M. (1984) Antibody against GABA: specificity studies and immunocytochemical results. *Proc. Natl Acad. Sci. USA* **81**, 3888–3892
20. Campistron, G., Buijs R.M., and Geffard, M. (1986) Specific antibodies against aspartate and their immunocytochemical applications in the rat brain. *Brain Res.* **365**, 179–184
21. Kato, K., Naoe, T., Hiraiwa, A., Namikawa, R., Suzuki, S., Yamada, K., and Shiku, H. (1985) Production and analysis of HH 10 monoclonal antibodies reactive to immature hematopoietic cells and their use in monitoring acute leukemia cells. *Jpn. J. Cancer Res.* **76**, 524–531
22. Fujiwara, K., Araki, M., Kitagawa, T., and Inoue, Y. (1993) A new enzyme-linked immunosorbent assay (ELISA) for studying immunocytochemical procedures using an antiserum produced against spermidine as a model. *Histochemistry* **99**, 477–483
23. Fujiwara, K., Kitagawa, T., Inoue, Y., and Alonso, G. (1997) Monoclonal antibodies against glutaraldehyde-conjugated histamine: application to immunocytochemistry. *Histochem. Cell Biol.* **107**, 39–45
24. Clements, J.R. and Beitz, A.J. (1985) The effects of different pretreatment conditions and fixation regimens on serotonin immunoreactivity: a quantitative light microscopic study. *J. Histochem. Cytochem.* **33**, 778–784
25. Peressini, S., Brusco, A., and Pecci Saavedra, J. (1984) Basis for the specificity anti-HT-like antisera in immunocytochemistry applied to the central nervous system. *Histochemistry* **80**, 597–602
26. Schipper, R.G., Jonis, J.A., Rutten, R.G.J., Tesser, G.I., and Verhofstad (1991) Preparation and characterization of polyclonal and monoclonal antibodies to polyamines. *J. Immunol. Methods* **136**, 23–30
27. Schipper, J. and Tilders, F.J.H. (1983) A new technique for studying specificity of immunocytochemical procedures: specificity of serotonin immunostaining. *J. Histochem. Cytochem.* **31**, 12–18
28. Geffard, M., Buijs, R.M., Seguela, O., Pool, C.W., and Le Moal, M. (1984) First demonstration of highly specific and sensitive antibodies against dopamine. *Brain Res.* **294**, 161–165
29. Fujiwara, K., Furukawa, K., Nakayama, E., and Shiku, H. (1994) Production and characterization of monoclonal antibodies against the polyamine: immunocytochemical localization in rat tissues. *Histochem. Cell Biol.* **102**, 397–404
30. Larsson, L.-I. (1988) *Immunocytochemistry, Theory and Practice*. CRC Press, Boca Raton, Florida